7482 *Biochemistry* **2009,** *48,* 7482–7491
DOI: 10.1021/bi9009659

BIOCHEMISTRY
including biophysical chemistry & molecular biology
Article

Acrylamide Quenching of Trp Phosphorescence in Liver Alcohol Dehydrogenase: Evidence of Gated Quencher Penetration

Giovanni B. Strambini* and Margherita Gonnelli

Consiglio Nazionale delle Ricerche, Istituto di Biofisica, 56124 Pisa, Italy

Received June 9, 2009; Revised Manuscript Received July 10, 2009

ABSTRACT: Notwithstanding the relevance of their biological function, slow motions in proteins, beyond the microsecond range, are still poorly understood and often elusive. We propose that acrylamide quenching of Trp phosphorescence of deeply buried residues, when extended over the entire accessible range of lifetime measurements ($\tau > 10\ \mu s$), may help to unveil low-frequency protein motions that allow penetration of solute into the protein interior. The work examines in some detail acrylamide quenching of Trp phosphorescence in a model protein (liver alcohol dehydrogenase) over an extended submillimolar to molar acrylamide concentration range. The results, which encompass a $>10^4$-fold variation in the quenching rate, provide the first evidence of a downward-curving lifetime Stern−Volmer plot, indicative of a nonlinear dependence of the quenching rate on the quencher concentration. From an analysis of saturation effects in terms of a protein-gated acrylamide diffusion mechanism, we infer two main routes for acrylamide to penetrate the globular fold and come into the proximity of internal W314: a low-frequency gate [36 s^{-1} (at 25 °C)] tentatively assigned to partial opening of the dimer interface and a higher-frequency one (11800 s^{-1}) tentatively assigned to a channel blocked by the side chains of V276 and L307. These motions are sharply inhibited in the rigid protein complexes formed with the coenzyme NAD^+ and the coenzyme analogue adenine diphosphate ribose, as well as by the frictional drag of the solvent in viscous glycerol solutions, evidence that rules out an alternative quenching mechanism involving acrylamide binding to the protein.

The growing interest in the study of protein dynamics draws from the general belief that for these biological macromolecules flexibility and function are intimately correlated. Evidence indicating that slow collective motions underlying the transition between conformational substates in the slow time domain (10^{-7}−10^0 s) are directly linked to enzymatic catalysis, signal transduction, and protein−protein interactions is accumulating (*1*−*5*). However, despite their relevance to biological function, slow motions beyond the microsecond range are still poorly understood and often elusive when they involve transitions to rarely populated states (*1*, *6*).

The diffusion of solutes through generally compact globular folds, requiring transient formation of channels or the opening of gates of commensurate size, has long been proposed as a means of analyzing structural fluctuations over a wide range of frequencies and amplitudes. One approach is based on fluorescence and phosphorescence quenching of internal Trp residues by added small solutes, historically one of the first techniques to provide information about the flexibility of these macromolecules (*7*−*10*). Quenching studies measure the luminescence lifetime (τ) as a function of quencher concentration ([Q]) and evaluate the bimolecular quenching rate constant (kq) from the gradient of the Stern−Volmer plot

$$1/\tau = 1/\tau_0 + kq[Q]$$

where τ_0 is the unperturbed lifetime. It is generally agreed that small diatomic molecules (e.g., O_2, NO, and CO) penetrate readily the protein matrix and that the reduction of up to 3−4 orders of magnitude in the phosphorescence quenching rate constant [kq(protein)/kq(solvent)] reflects hindered diffusion through compact regions of the globular fold. For larger quenchers like acrylamide (M_w = 71), however, migration is expected to require transient formation of relatively big channels and, indeed, the quenching rate is much more strongly inhibited relative to those of diatomic molecules, the kq(protein)/kq(solvent) ratio falling in the range from 10^{-10} to 10^{-4} (*11*). It has also been suggested that acrylamide cannot penetrate the protein fold even on the long millisecond to second time scale of phosphorescence and that the quenching reaction involves either long-range through-space interactions between the chromophore and acrylamide in the solvent or partial unfolding transitions bringing the buried chromophore into the proximity of the aqueous phase (*12*, *13*). More recently, however, numerous examples of sharp modulation of the quenching rate by stabilizing or destabilizing additives, binding of metal ions and cofactors, and the application of hydrostatic pressure have entailed a direct correlation between the magnitude of kq(protein) and protein flexibility that tends to rule out long-range quenching mechanisms (*11*, *14*, *15*). Whether the reaction involves internal migration of acrylamide or partial unfolding transitions bringing Trp to the aqueous interface, the process requires structural fluctuations of a relatively large amplitude that presumably occur in the microsecond time domain or slower. The process, generally termed protein-gated quencher diffusion, would be limited by the gate frequency (v_g) ($kq[Q] \leq v_g$) and would give rise to a downward-curving Stern−Volmer plot with an evident saturation effect. Until now, quenching studies have commonly explored a limited [Q] range, sufficient to reduce

*To whom correspondence should be addressed: CNR, Istituto di Biofisica, Area della Ricerca, via Moruzzi 1, 56124 Pisa, Italy. Telephone: +39 050 315 3046. Fax: +39 050 315 2760. E-mail: strambini@pi.ibf.cnr.it.

 Published on Web 07/13/2009

the lifetime to approximately one-tenth of τ_0, and within this range, the Stern−Volmer plot has been found to be essentially linear. For a protein with a phosphorescence lifetime τ_0 of 1 s, it means quenching rates of up to 10 s^{-1}. It is possible that the limited range of quenching rates explored and/or the occurrence of higher gate frequencies has as yet precluded the emergence of saturation effects in the Stern−Volmer plot. To exploit the full potential of phosphorescence lifetime measurements ($\tau_0 > \tau > 10$ μs) to unveil low-frequency structural fluctuations, this work examines in great detail acrylamide quenching of Trp phosphorescence in a model protein [horse liver alcohol dehydrogenase (LADH)][1] extending the [Q] range from submillimolar to the molar upper limit imposed by the quencher inner filter. The results, which encompass a $>10^4$-fold variation of the quenching rate, provide the first evidence of a downward-curving lifetime Stern−Volmer plot. Data analysis in terms of a gating mechanism indicates two main routes for acrylamide migration that, at 25 °C, are governed by gate frequencies of 36 and 11800 s^{-1}, respectively. These motions are sharply inhibited in the protein complexes with the coenzyme or coenzyme analogue as well as by the frictional drag of the solvent in viscous glycerol solutions, findings that rule out alternative quenching mechanisms based on long-range interactions with acrylamide in the solvent or bound to the protein surface.

MATERIALS AND METHODS

All chemicals were of the highest purity grade available from commercial sources and unless specified to the contrary were used without further purification. Acrylamide (99.9% electrophoretic purity) was from Bio-Rad Laboratories (Richmond, CA). Tris(hydroxymethyl)aminomethane (Tris), spectral grade glycerol, and NaCl Suprapur were from Merck (Darmstadt, Germany). The protein horse liver alcohol dehydrogenase (LADH), NAD^+, ADPR, and pyrazole were purchased from Sigma Chemical Co. (St. Louis, MO). Water was purified by reverse osmosis (Milli-RX 20, Millipore, Billerica, MA) and subsequently passed through a Milli-Q Plus system (Millipore Corp., Bedford, MA).

Concentrated LADH stock solutions were prepared monthly by dialysis of the commercial suspension against 100 mM Tris-HCl buffer and 50 mM NaCl (pH 7) and stored at 4 °C. Acrylamide stocks were prepared daily by dilution of the 5.63 M commercial supply in 10 mM Tris-HCl buffer (pH 7). In all samples, the final protein concentration was maintained around 4 μM, except in the ternary complex with NAD^+ and pyrazole where it was 8 μM. The buffer was 10 mM Tris-HCl (pH 7) throughout the process. The complexes of LADH with ADPR and with NAD^+ and pyrazole were formed simply by adding the reagents to the protein solution to a final concentration of 430 μM for ADPR, 9 μM for NAD^+, and 10 mM for pyrazole.

For phosphorescence measurements in fluid solutions, it is paramount to rid the solution of all O_2 traces. Protein samples placed in appositely constructed, 5 mm × 5 mm, quartz cuvettes were deoxygenated by repeated cycles of mild evacuation followed by inlet of pure nitrogen as previously described (*16*). In the case of glycerol solutions, the time of deoxygenation was prolonged from 10 to 30 min and the sample temperature increased to 35 °C to accelerate gas exchange.

[1]Abbreviations: LADH, horse liver alcohol dehydrogenase; ADPR, adenine diphosphate ribose.

Phosphorescence Measurements. Fluorescence and phosphorescence spectra and phosphorescence decays were all measured with pulsed excitation (λ_{ex} = 295 nm) on a homemade apparatus (*16*) modified for implementation of spectral measurements by means of a CCD camera. Pulsed excitation was provided by a frequency-doubled Nd/Yag-pumped dye laser (Quanta Systems, Milano, Italy) with a pulse duration of 5 ns and a typical energy per pulse of 0.5−1 mJ. For spectral measurements, the emission was collected at 90° from the excitation and dispersed by a 0.3 m focal length triplet grating imaging spectrograph (SpectraPro-2300i, Acton Research Corp., Acton, MA) with a band-pass of 2.0 nm. The emission was monitored by a back-illuminated 1340 pixel × 400 pixel CCD camera [Princeton Instruments Spec-10:400B (XTE), Roper Scientific Inc., Trenton, NJ] cooled to −60 °C. We monitored phosphorescence decays by collecting the emission at 90° from vertical excitation through a filter combination with a transmission window of 405−445 nm (WG405, Lot-Oriel, Milan, Italy; plus interference filter DT-Blau, Balzer, Milan, Italy). The photomultiplier (EMI 9235QA, EMI, Middlesex, U.K.) was protected against fatigue from the strong excitation/fluorescence pulse by either a gating circuit or a mechanical chopper synchronized to the laser trigger, which closed the emission slit during the excitation pulse. The time resolution of the latter option depends on the chopper speed and for the experiments reported here was kept constant at 20 μs. The photocurrent was amplified by a current-to-voltage converter (SR570, Stanford Research Systems, Stanford, CA) and digitized by a 16 bit high-speed (1.25 MHz) multifunction data acquisition board (NI 6250 PCI, National Instrument Italy, Milan, Italy) supported by LABVIEW software capable of averaging multiple sweeps. Typically, fewer than 20 sweeps were sufficient for a good signal-to-noise ratio even for the shortest decays. Prompt fluorescence was simultaneously collected through a 310−375 nm band-pass filter combination (WG305 nm plus Schott UG11) and detected by a UV-enhanced photodiode (OSD100-7, Centronics, Newbury Park, CA). An analogue circuit was used to integrate the photocurrent, and its output was digitized and averaged by a multifunctional board (NI 6250 PCI, National Instrument Italy) utilizing LABVIEW. The prompt fluorescence intensity was used to account for possible variations in the laser output between measurements as well as to obtain fluorescence-normalized phosphorescence intensities. All phosphorescence decays were analyzed in terms of discrete exponential components by a nonlinear least-squares fitting algorithm (DAS6, Fluorescence decay analysis software, Horiba Jobin Yvon, Milan, Italy).

For each acrylamide concentration, at least three independent samples were analyzed and the reported results represent the mean lifetime value. The reproducibility of phosphorescence lifetime measurements was generally better that 5%.

Acrylamide Quenching Experiments. Acrylamide quenching experiments were conducted by measuring the phosphorescence lifetime of LADH as a function of acrylamide concentration in solution (*11*). The bimolecular quenching rate constant (kq) was evaluated from the gradient of the Stern−Volmer plot

$$1/\tau = 1/\tau_0 + \mathrm{kq}[\mathrm{acrylamide}]$$

where τ_0 is the unperturbed lifetime. The phosphorescence emission of LADH is intrinsically heterogeneous and requires

two lifetime components to adequately fit the decay (for the quencher free decay at 25 °C, $\tau_1 = 125$ ns, $\tau_2 = 430$ ns, and $\alpha_1 = 0.13$), the lifetime multiplicity reflecting the presence of more than one stable conformation of the macromolecule (*17*). The τ heterogeneity is partly attenuated on acrylamide quenched samples, an indication that the conformers have similar accessibilities to acrylamide quenching. For the free protein and for the coenzyme complexes, lifetime Stern−Volmer plots were all constructed from the intensity-averaged lifetime (*18*) ($\tau = \sum \alpha_i \tau_i^2 / \sum \alpha_i \tau_i$) obtained by a two-component fit of the decay. The variation of α_i and τ_i as a function of acrylamide concentration in a typical experiment is shown in the Supporting Information.

Quenching Models. Quenching of the luminescence of buried Trp residues in proteins by small solutes (Q) in solution has been analyzed in terms of mechanisms that involve either diffusion of Q to the protein surface followed by long-range interactions with the buried chromophore or diffusive penetration of Q through the protein matrix to its proximity. Pertinent analytical expressions for the quenching rate, obtained by solving Fick's diffusion equation applying radiation boundary conditions, and their application range in the realm of protein phosphorescence have been discussed in detail previously (*19*). Briefly, when a transient time-dependent term arising from Q molecules already in the proximity of the chromophore at the instant of excitation is neglected, the steady-state quenching rate is given by

$$\text{rate} = \text{kq}[\text{Q}] \quad \text{with} \quad \text{kq} = (k_\text{D} k_\text{I})/(k_\text{D} + k_\text{I}) \qquad (1)$$

where k_D [$= 4\pi a D$ ($\text{cm}^2\ \text{s}^{-1}$)] is the Smoluchowski diffusion-controlled rate constant, k_I [$4\pi a^2 B$ ($\text{cm}^2\ \text{s}^{-1}$)] is the diffusion-independent maximum rate constant. D is the sum of the separate diffusion coefficients of Q and protein in solution. B is an interaction strength parameter related to the distance dependence of the quenching interaction, $k(r)$, and a is the distance of the closest approach between Q and the chromophore. Depending on which of the two constants is smaller, the process goes from the diffusion-controlled regime ($k_\text{D} \ll k_\text{I}$, $\text{kq} \propto D$) to the reaction-controlled regime ($k_\text{D} \gg k_\text{I}$, $\text{kq} = k_\text{I}$), where kq is independent of diffusion. Because of the long lifetime of the excited triplet state and the generally weak, short-range nature of its interactions with Q, the latter regime is believed to generally apply to quenching of protein phosphorescence in an ordinary aqueous solution (*12*, *13*). For Q relegated to the aqueous phase and an exponential electron exchange interaction [$k(r) = k_0 \exp(-r/\lambda)$], it was shown that the bimolecular rate constant decreases exponentially with distance a between the chromophore and aqueous interface, according to (assuming an essentially flat protein surface) (*20*)

$$\text{kq}(a) = 2\pi N k_0 \times 10^{-3} (\lambda a^2 + 2\lambda^3) \exp(-a/\lambda)\ \text{M}^{-1}\ \text{s}^{-1} \qquad (2)$$

where N is Avogadro's number.

Instead, for diffusive penetration of Q across a protein shell of thickness T, characterized by a diffusion constant $D_\text{s} \ll D$, the process is bound to be under diffusion control, and in such a case, the rate constant assumes the form of a corrected Smoluchowski equation (*19*)

$$\text{kq} = 4\pi a D_\text{s} (1 + a/T) \qquad (3)$$

where now a is the radius of the impermeable protein core surrounding the chromophore.

Equations 1−3 contemplate a linear dependence of the quenching rate on [Q], i.e., a linear lifetime Stern−Volmer plot. The transient time-dependent term would cause a positive deviation to the intensity Stern−Volmer plot and introduce a short-lived component into the emission decay.

Equation 1 has the form expected for a steady-state rate in a system of two sequential processes, the first of which is the diffusion of Q into the vicinity of the chromophore followed by the reaction that quenches the excited state. Here, we adopt an analogous scheme to derive a simple expression for kq for the special case in which migration of Q to within interaction range of the excited triplet state requires a major structural fluctuation, i.e., the opening of a "gate", be it internal within the protein matrix or open to the solvent [more elaborate treatments can be found elsewhere (*21*−*23*)]. Schematically, it is assumed that the macromolecule is in rapid equilibrium between closed (Pc) and open (Po) conformations and that quenching occurs exclusively in the open conformation, the latter representing a small fraction of the protein population ($k_\text{o} \ll k_\text{c}$).

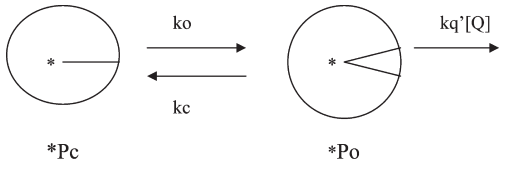

In this scheme, the rate of quenching is

$$\text{kq}[\text{Q}] = \text{fokq}'[\text{Q}] \qquad (4)$$

where $\text{fo} = [*\text{Po}]/([*\text{Po}] + [*\text{Pc}]) \approx [*\text{Po}]/[*\text{Pc}]$ is the fraction of excited proteins in the quenchable, open gate conformation. kq is the experimental quenching rate constant, while $\text{kq}' = k_\text{D} k_\text{I}/(k_\text{I} + k_{-\text{D}})$ is the quenching rate constant characteristic of the open state. By analogy to eq 1, k_D is the constant for diffusion of Q across the gate and k_I the maximum reaction rate in the open conformation. We shall also assume that the unquenched phosphorescence lifetime, τ_0, is similar for closed and open protein states and that it is long relative to the open−closed equilibrium. Then, at time zero

$$\text{fo} = \text{ko}/\text{kc}$$

and

$$\text{kq}(0) = (\text{ko}/\text{kc})\text{kq}' = \text{ko}/\sigma \qquad (5)$$

where

$$\sigma = \text{kc}/\text{kq}'$$

At $t > t_\text{equil}$, steady-state conditions apply and, therefore

$$\text{d}[*\text{Po}]/\text{d}t = \text{ko}[*\text{Pc}] - (\text{kq}'[\text{Q}] + \text{kc})[*\text{Po}] = 0$$

$$\text{fo} = [*\text{Po}]/[*\text{Pc}] = \text{ko}/(\text{kq}'[\text{Q}] + \text{kc})$$

whence

$$\text{kq}(t > t_\text{eq}) = \text{kq}'\text{ko}/(\text{kq}'[\text{Q}] + \text{kc}) = \text{ko}/([\text{Q}] + \sigma) \qquad (6)$$

σ represents the quencher concentration corresponding to the midpoint saturation of the gate. In this framework, kq depends on the quencher concentration and approaches its maximum value $\text{kq}_\text{max} = \text{ko}/\sigma$ at low values of [Q]. At high values of [Q], such that $[\text{Q}] > \sigma$, kq approaches

$$\text{kq} = \text{ko}/[\text{Q}]$$

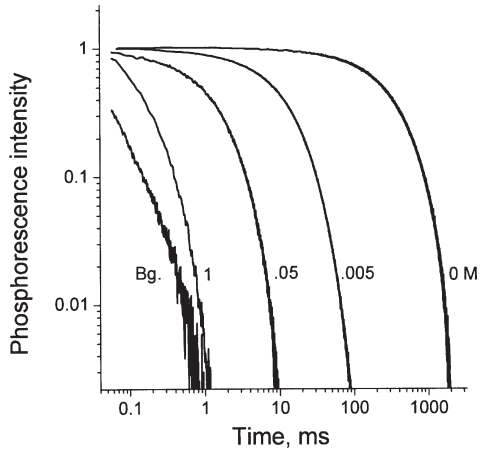

FIGURE 1: Trp phosphorescence decay of LADH at selected acrylamide concentrations in the 0−1 M range, at 25 °C. The protein concentration is 4 μM in 10 mM Tris (pH 7). λ_{ex} = 295 nm. The signals represent the average of 2−20 pulses. The blank control at 1 M acrylamide, Bg, is also included.

and the quenching rate becomes independent of Q

$$kq[Q] = ko \approx v_g$$

namely, at a high concentration the quenching rate is limited by the gate opening rate, ko (or gate frequency v_g). Above, we noted that kq is also time-dependent, decreasing from its initial value of ko/σ to the equilibrium value of $ko/([Q]+\sigma)$. This implies that the phosphorescence decay initially is more rapid and therefore nonexponential.

It must be pointed out that an analogous hyperbolic [Q] dependence of the quenching rate arises for a quenching scheme in which Q binds reversibly to a protein site within the interaction range of the chromophore and in the bound state quenches the emission at a rate $k(r_i')$, r_i' being the quencher−chromophore separation at the ith binding site. By analogy to eq 4, the contribution to the quenching rate by a single binding site is

$$kq[Q] = fbk(r') = k(r')[1/(K_d/[Q] + 1)] \quad (7)$$

where $fb = 1/(K_d/[Q] + 1)$ is the Q-bound protein fraction and K_d the corresponding dissociation constant. Comparison of the quenching rates obtained from eqs 6 and 7, after suitable rearrangement

$$ko[1/(\sigma/[Q] + 1)] \text{ and } k(r')[1/(K_d/[Q] + 1)]$$

shows that in the binding scheme $k(r')$ is equivalent to the gate opening rate, ko, and that K_d is equivalent to σ. Thus, the [Q] dependence of the rate by itself cannot discriminate between these two alternative mechanisms.

RESULTS

Acrylamide Quenching of LADH Phosphorescence over an Extended Concentration Range. The room-temperature phosphorescence of LADH, which is due exclusively to Trp-314 deeply buried at the dimer subunit interface, is readily quenched by acrylamide in solution (*11*). Figure 1 shows the effect of selected acrylamide concentrations on the phosphorescence decay of 4 μM LADH in 10 mM Tris (pH 7) at 25 °C. Across the 0−1 M concentration range, the intensity average phosphorescence lifetime (τ) decreases from ~400 ms to 170 μs, which is more than 2000-fold. Quencher concentrations of > 1 M are not practical for the strong inner filter of acrylamide. Blank controls indicate that the background emission is not negligible during the initial 200−300 μs of the decay (figure 1) and, therefore, needed to be subtracted from the decay of concentrated samples. Another concern with concentrated solutions is the possibility of acrylamide polymerization, which is favored by warm temperatures as well as by the generation of free radicals such as Trp photoproducts, which are invariably formed during sample excitation. Pertinent controls obtained by varying the excitation dose confirmed that even at twice the normal dose no effect was detected in the phosphorescence lifetime of concentrated samples or in the viscosity of the solution that is sensitive to polymerization.

Figure 2 is the lifetime Stern−Volmer plot obtained at 25 °C, and in supercooled solutions at −5 °C, upon variation of the acrylamide concentration from 2×10^{-4} to 1 M, in roughly constant steps. At both temperatures, the plot exhibits significant negative deviations from linearity, the downward curvature being evident even in the millimolar concentration range, although less pronounced than at high concentrations. These findings explain also the reason why previous quenching studies of LADH reported linear plots (*11*, *15*). They were conducted over the 0−1 mM acrylamide concentration range, sufficient to reduce by up to 10-fold the unperturbed lifetime, and within this limited range, Figure 2 shows that the plot is practically linear. Over this range, the gradient yields a kq value of 2.1×10^4 M^{-1} s^{-1}, at 25 °C, which is in accord with the value of 1.2×10^4 M^{-1} s^{-1} reported previously at 20 °C (*11*).

The decrease in kq at high acrylamide concentrations, as obtained by dividing the quenching rate by [Q], is illustrated in Figure 3. At both temperatures, we observe a biphasic decrease in kq that, overall, amounts to a factor of 3.7 at 25 °C and a factor of 10 at −5 °C. We have analyzed the dependence of kq on the acrylamide concentration in terms of protein-gated diffusion involving two distinct gated pathways (eq 6). The goodness of the fit to a two-gate quenching model is shown in Figure 4, and the resulting gate frequencies, v_i, with the respective gate saturation midpoints, σ_i, are collected in Table 1. According to this analysis, acrylamide accessibility to Trp-314 is dominated by two distinct structural fluctuations having frequencies in the range of 36 and 11800 s^{-1}, with saturation midpoints around 0.004 and 1 M, respectively. The maximum relative contribution of each gate to the overall quenching rate, v_i/σ_i, is similar at 25 °C, whereas at −5 °C, the fast gate is twice less efficient than the slow gate (Table 1).

As mentioned in the section about quenching models, the downward curvature of the Stern−Volmer plot can in principle be ascribed equally well to an alternative mechanism based on binding of acrylamide to protein sites within interaction distance, r_i, of Trp-314. To discriminate between these two mechanisms, we performed quenching experiments under experimental conditions in which the binding affinity for acrylamide is presumably kept constant if not increased whereas the structural flexibility of the protein, crucial in a gated model, is strongly reduced either by formation of complex with the coenzyme or by increasing solvent viscosity.

Acrylamide Quenching of the LADH−ADPR and LADH−NAD−Pyrazole Complexes. The crystallographic structures of the complexes described above show that the large cleft separating the catalytic domain from the coenzyme binding domain is closed in the ternary NAD complex but remains open, as in the free protein, in the complex with the coenzyme analogue

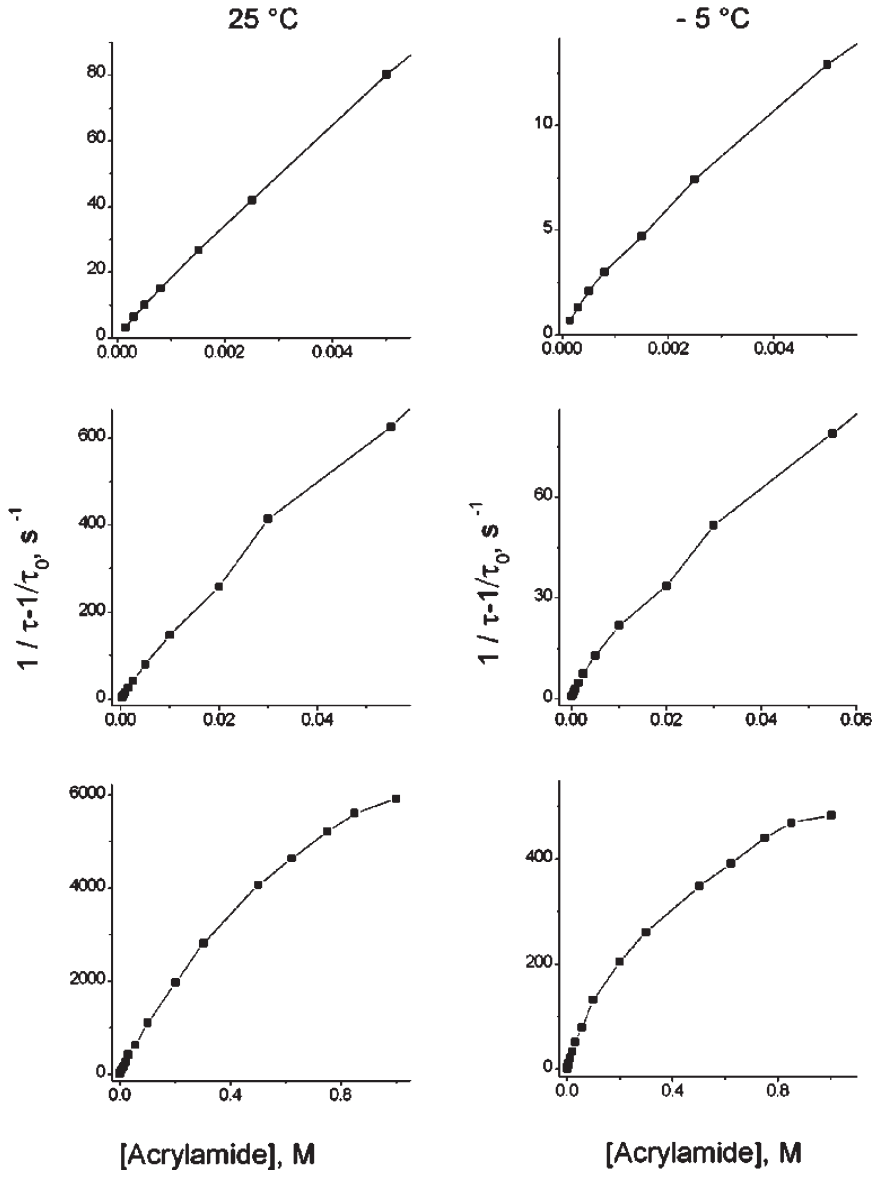

FIGURE 2: Lifetime Stern−Volmer plots for the quenching of LADH phosphorescence by acrylamide, at 25 °C and in supercooled solutions at −5 °C. The three panels represent expanded concentration scales. τ_0 = 0.42 s at 25 °C, and τ_0 = 2.47 s at −5 °C. Each point is the mean value of at least three separate determinations. Deviations from the mean are typically smaller than 5%. Other conditions are as described in the legend of Figure 1.

ADPR (*24*, *25*). In either case, on the basis of the *B*-factors, the increase in τ_0 (*26*), and the enhanced thermal stability(*27*), both complexes are structurally more rigid relative to the free protein. In the region of the dimer interface, where Trp-314 is located, the protein structure is not changed by formation of a complex.

Figure 5 includes the lifetime Stern−Volmer plots obtained with the complexes described above, at 25 and −5 °C. The samples refer to 4 μM LADH and 450 μM ADPR in 10 mM Tris (pH 7) for the 1:2 LADH−ADPR binary complex and 8 μM LADH, 9 μM NAD^+, and 10 mM pyrazole in 10 mM Tris (pH 7) for the 1:1 ternary complex. A higher protein concentration in the NAD^+ complex served to compensate for the partial quenching of Trp-314 emission by the coenzyme (*26*). Relative to that of the free protein, the rate of quenching is significantly reduced in the coenzyme complexes, and now the Stern−Volmer plot is essentially linear in the quencher concentration range throughout the process. A positive deviation from linearity is observed only in the case of the LADH−ADPR complex at 25 °C and at the highest quencher concentration. Considering the relatively weak affinity of the binary complex, it is possible that molar acrylamide induces partial ADPR dissociation and that a fraction of LADH is free or in a 1:1 stoichiometry, forms that are more strongly quenched than the 1:2 complex.

From the perspective of gated acrylamide migration, a linear plot implies that practically only one of the two gates is operative and that its σ is beyond 1 M acrylamide. In view of the remarkable deceleration of the reaction, we presume that in the complexes the slow gate is virtually blocked on the centisecond time scale while the fast gate is ~10 times slower. The increase in σ = kc/kq′ to beyond 1 M would suggest that the "open" conformation has also become less accessible to quenching, relative to the free protein.

The second-order rate constant derived from a linear fit of these plots is reported in Table 2. Relative to the kq_{max} of the free protein, the rate constant at 25 °C has been reduced 18-fold in the ADPR complex and 25-fold in the NAD complex. The inhibition factor is more than twice as large at −5 °C. Thus, the accessibility to acrylamide quenching is drastically reduced in both open

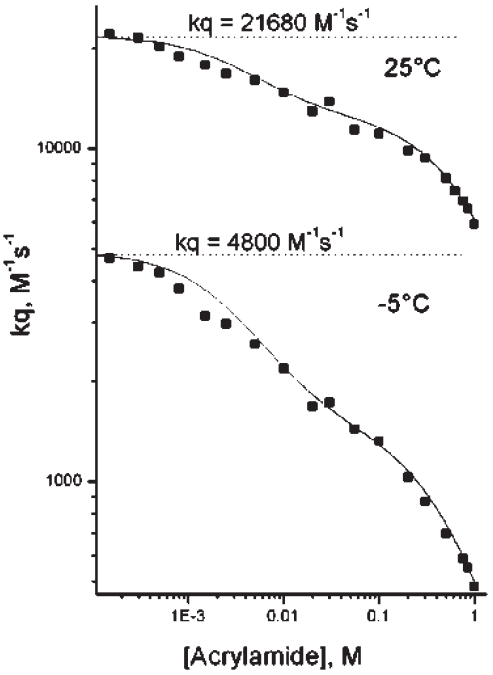

FIGURE 3: Dependence of the bimolecular quenching rate constant, kq, on acrylamide concentration as obtained by dividing the data from Figure 2 by the acrylamide concentration. The solid line through the points is the best fit of the data to a two-gate mechanism (eq 6 and Figure 4). The dashed line represents the value of kq expected for a linear dependence of the rate on acrylamide concentration.

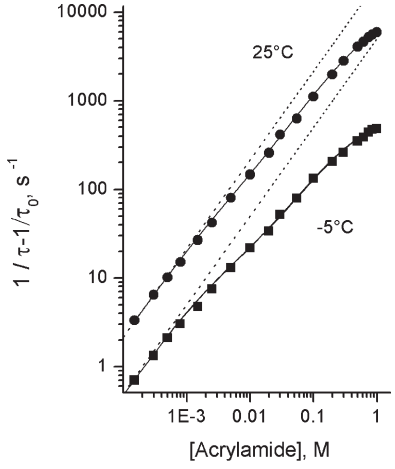

FIGURE 4: Fits of the quenching rate (the data from Figure 2) in terms of a two-gate mechanism (solid line) with parameters v_i and σ_i reported in Table 1. The dashed line shows the deviation of the data from a linear dependence of the rate.

Table 1: Gate Parameters Derived for Acrylamide Quenching of LADH at Selected Temperatures

T (°C)	ko (s^{-1})	σ (mM)	ko/σ	$\Delta H^{\ddagger}$(ko) (kcal/mol)
−5	10.8 ± 7	3 ± 3	3.6	6.4
	742 ± 52	520 ± 10	1.4	14.7
25	36 ± 18	4 ± 3	9.0	
	11800 ± 380	950 ± 55	12.4	

(ADPR) and closed (NAD^+) coenzyme complexes. The activation enthalpy of kq, $\Delta H^{\ddagger}$(kq), inferred from the two-point Arrhenius plot over a 30 °C temperature interval, shows an

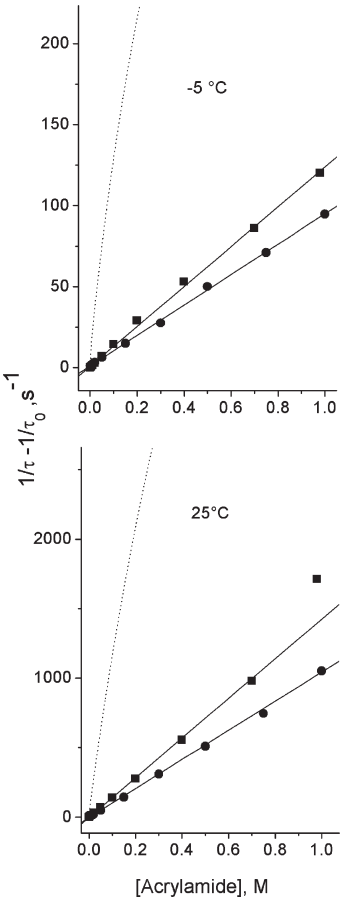

FIGURE 5: Lifetime Stern−Volmer plots for acrylamide quenching of binary (■) LADH−ADPR and ternary (●) LADH−NAD^+−pyrazole complexes, at 25 and −5 °C. τ_0 = 0.98 and 2.47 s for the binary complex and τ_0 = 0.51 and 1.57 s for the ternary complex at 25 and −5 °C, respectively. The line drawn through the points is a linear fit of the data. The quenching rate of LADH under the same conditions is included for the sake of comparison (dashed line).

increase of ~4 kcal/mol from the free protein to the complexes (Table 2). While these findings corroborate a gated mechanism in which conformational fluctuations required for quencher access to Trp-314 are effectively decelerated in the more rigid protein complexes, they are hardly consistent with an external quenching mechanism.

Effect of a Viscous Glycerol/Buffer Mixture on the Rate of Acrylamide Quenching of LADH. Acrylamide quenching of LADH phosphorescence was examined in a glycerol/buffer mixture (68:32, w/w) up to 1 M acrylamide, at both 25 and −5 °C. Blank controls showed a non-negligible emission from the organic solvent during the first millisecond of the decay, although it is considerably attenuated and shorter-lived in the presence of acrylamide. A blank correction to the protein emission was required only for concentrated samples at 25 °C. Quenching impurities in the organic solvent are also presumably responsible for the slight shortening of the protein phosphorescence lifetime in a glycerol/buffer mixture, reducing τ from 0.42 to 0.38 s at 25 °C and from 2.27 to 1.76 s at −5 °C.

The acrylamide quenching rate in this solvent is reported in Figure 6, and the derived parameters are collected in Table 2. As for the complexes, the Stern−Volmer plot is essentially linear, even if the slope of the log−log plot from 0.001 to 1 M acrylamide is somewhat smaller than 1, namely, 0.92 at 25 °C and 0.90 at −5 °C. The gradient of a linear fit yields kq values of 3.2×10^3 M^{-1} s^{-1} at

Table 2: Effect of Glycerol and Formation of the Coenzyme Complex on the Bimolecular Acrylamide Quenching Rate Constant of LADH, at −5 and 25 °C

sample	kq_{-5} (M^{-1} s^{-1})	kq_{25} (M^{-1} s^{-1})	R_{-5}[a]	R_{25}	η_{-5}/η_{25}[b]	$\Delta H^{\ddagger}$(kq) (kcal/mol)
LADH	4800[c]	21700[c]	1	1	2.5	8.5
LADH with glycerol (68%)	107	3200	45	7	5.3	17.6
LADH−ADPR	108	1200	45	18	2.5	12.9
LADH−NAD−pyrazole	94	870	51	25	2.5	12.6

[a] $R = kq[LADH]/kq$. [b] $\eta_{25} = 0.9$ cP in water, and $\eta_{25} = 16$ cP in 68% glycerol ($\eta_g/\eta_w = 17.7$); $\eta_{-5} = 2.25$ cP in water, and $\eta_{-5} = 80$ cP in 68% glycerol ($\eta_g/\eta_w = 35.5$). [c] kq_{max} obtained from the gradient in the low concentration end of the Stern−Volmer plot.

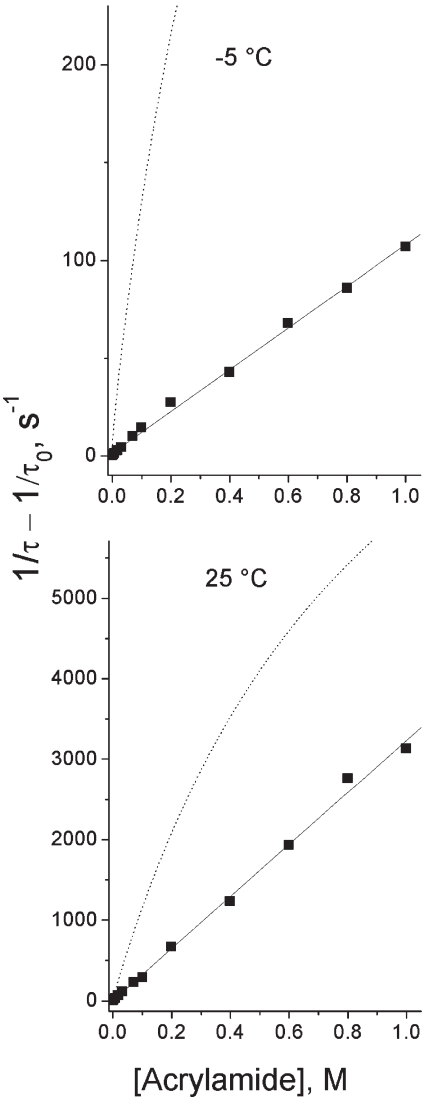

FIGURE 6: Lifetime Stern−Volmer plot for the quenching of LADH phosphorescence in a glycerol/buffer mixture (68:32, w/w), at 25 and −5 °C. $\tau_0 = 0.38$ and 1.98 s, respectively. The line drawn through the points is a linear fit of the data. The quenching rate of LADH in buffer is included for the sake of comparison (dashed line).

25 °C and 1.1×10^2 M^{-1} s^{-1} at −5 °C. These values correspond to 7- and 45-fold reductions in kq relative to that of buffer, respectively, and to an ~2-fold increase in the activation enthalpy (17.6 kcal/mol). Relative to that of water, the viscosity of glycerol solutions increased 17.7-fold at 25 °C and 35.5-fold at −5 °C. These findings suggest an inverse dependence of kq on solvent viscosity that is to be expected when the quenching reaction involves structural fluctuations in the protein. Besides direct viscosity-dependent kinetic effects on the quenching rate, the overall process may be further inhibited by the selective cosolvent stabilization of closed, compact protein conformers as glycerol is known to promote protein folding (*28*). On the other hand, strong inhibition of acrylamide quenching in glycerol solutions is not consistent with a binding model as that would require a drastic decrease in binding affinity whereas there is evidence to the contrary, namely, that the cosolvent tends to strengthen binding of acrylamide to proteins (*29*).

DISCUSSION

Trp-314 of LADH is buried at the dimer interface, shielded from the solvent by a compact protein shell with a thickness *a* of ≥4.5 Å. It exhibits an acrylamide quenching constant of 2.1×10^4 M^{-1} s^{-1}, at 25 °C, which is ~5 orders of magnitude smaller than that for solvent-exposed residues (*30*). In the crystal structure, there are no channels or crevices of commensurate size that could permit diffusion of a solute the size of acrylamide into the proximity of the aromatic ring. In a previous report, it was suggested that any contribution to the rate from through-space quenching by acrylamide in the solvent must be negligible as the rate estimated with the application of eq 2 is ~4 orders of magnitude smaller than the experimental value (*11*). Thus, it was concluded that fluctuations about the equilibrium configuration of the macromolecule must occur to allow migration of the quencher through the protein matrix, and the reduction of kq relative to solvent-exposed residues was analyzed in terms of hindered diffusion by eq 3 [$kq(protein)/kq(water) \propto D_s/D$].

A key finding of this investigation is that when the acrylamide quenching rate is monitored over an extended concentration range it manifests saturation effects not contemplated in the classical relationships employed to describe luminescence quenching (eqs 1−3). Here, we propose that the negative deviation from the linear Stern−Volmer plot is a direct consequence of protein-gated acrylamide diffusion, as illustrated in the simple scheme above (Materials and Methods) and described by eq 6. Data analysis within this framework distinguishes two pathways: one characterized by a low-frequency gate ($\upsilon_1 \approx 40$ s^{-1}) that saturates relatively early, in the concentration range of 10 mM, and the other involving a higher-frequency gate ($\upsilon_2 \approx 12000$ s^{-1}) that saturates late in the molar concentration range. In the low concentration end, the contribution of each gate to the overall rate (ko/σ) is similar at 25 °C but becomes asymmetric at −5 °C, with a net prevalence of the slow gate. The reason is that protein motions underlying the fast gate (υ_2) exhibit a larger activation barrier, ~15 kcal/mol, as compared to 6.4 kcal/mol for those involved in υ_1. The saturation midpoints, on the other hand, are relatively independent of temperature.

As noted above, however, there is another formally equivalent mechanism that leads to saturation effects, and that is reversible binding of acrylamide to protein sites within the interaction distance of Trp-314 (eq 7). From this perspective, the rate would

be the sum of contributions from quencher molecules bound to two distinct sites with affinities K_{d1} of 4 mM and K_{d2} of 1 M and corresponding through-space rates $k(r_1)$ of 40 s^{-1} and $k(r_2)$ of 1.2×10^4 s^{-1}. From the distance dependence of the interaction [$k(r) = 2 \times 10^{10}$ exp($-r$/0.29) s^{-1}, where r (angstroms) is the quencher chromophore separation beyond van der Waals contact (*11*)], we infer that these sites would be separated from the indole ring of Trp-314 by a distance r_1 of 5.7 Å and a distance r_2 of 4.1 Å, which is possible only if they are very close to the dimer interface. Although very weak binding of acrylamide has been observed in numerous proteins (*29*), and external quenching through binding interactions can potentially account for both the magnitude of the quenching rate and its nonlinear behavior, specific tests rule out this mechanism.

A key feature of the gating mechanism is that, as opposed to binding, it relies on segmental protein motions and therefore is intimately connected to structural flexibility. Any factor affecting protein dynamics is bound to alter gate frequencies and amplitudes in a predictable way. Conversely, in a binding mechanism, only alteration of the protein surface topology in the vicinity of the dimer interface, causing a change in the position (r_i) or number of binding sites, would affect the quenching rate. Multiple data discriminate between the two mechanisms and support the gating hypothesis. (i) The large, roughly 10-fold reduction in quenching rate in the coenzyme complexes is consistent with gating but not with binding. An invariant protein surface topology in the region of the subunit interface (*24*) does not contemplate large differences in either the number of acrylamide binding sites or their affinity. Further, any acrylamide molecules eventually displaced by the ligand from sites in the coenzyme−analogue binding region would lie more than 13 Å from W314, well beyond the interaction range, to have any consequence. On the other hand, various indicators of structural flexibility, such as the lengthening of the phosphorescence lifetime of W314 (*26*), smaller *B*-factors (*25*), and a greater thermal stability (*27*), attest that the macromolecule becomes more rigid in both the open complex with ADPR and the closed complex with NAD and pyrazole. The prediction is that conformational fluctuations required for quencher access to Trp-314 will effectively be slowed in the more rigid protein complexes. (ii) The significant decrease in the quenching rate in viscous glycerol solutions, 7-fold at 25 °C ($\eta_g/\eta_w = 17.7$) and 45-fold at −5 ($\eta_g/\eta_w = 35.5$), suggests a direct link between kq and solvent viscosity. The solvent viscous drag is expected to dampen structural fluctuations in the protein (ko and kc) (*31*, *32*) and therefore slow gated acrylamide penetration. Above and beyond direct viscosity-dependent kinetic effects on the quenching rate, in a gated perspective the process may be further inhibited by the selective stabilization of closed, compact protein conformers by a cosolvent known to promote protein folding (*28*). On the other hand, there is evidence that glycerol tends to strengthen the binding of acrylamide to proteins, both in affinity and in the number of binding sites (*29*), which in a binding hypothesis would be expected to enhance the quenching rate. (iii) The relatively large and system-dependent activation barrier for the quenching rate, $\Delta H^{\ddagger}$(kq), is not consistent with external quenching. From eqs 6 and 7, we note that, depending on the mechanism, the activation enthalpy essentially refers to either ko or $k(r)$. For an electron exchange interaction, believed to underlie acrylamide quenching, the activation enthalpy of $k(r)$ is expected to be modest and rather insensitive to the medium (*33*), i.e., to be roughly constant among protein sites and protein systems. On the basis of acrylamide quenching of W59 in RNase T1, $\Delta H^{\ddagger}[k(r)]$ was inferred to be ≤5 kcal/mol (*11*). For LADH, we obtained $\Delta H^{\ddagger}$ values of 6.4 and 15 kcal/mol, which are quite different between the two sites, and in one case, the magnitude is 3 times larger than that predicted for $k(r)$. Also, the barrier is large, 12.7 kcal/mol, in the complexes and increases to 17.6 kcal/mol in viscous glycerol solutions. On the other hand, for gated diffusion, $\Delta H^{\ddagger}(\upsilon_i)$ represents the activation barrier of the structural fluctuation underlying the opening of the gate and, naturally, will vary considerably between alternative migration pathways. Barriers in the range of 10−20 kcal/mol are typical for large amplitude motions involving partial unfolding of the polypeptide. As one would expect, the height of these barriers is subject to be modulated by compaction of the globular fold, such as in the coenzyme complexes, and by solvent viscosity. (iv) In Table 1, we note an apparent correlation between gate frequency (υ_i) and midpoint saturation (σ_i). While in a gate model it is reasonable that a slower gate be saturated at lower quencher concentrations, no such link is anticipated between the parameters $k(r_i)$ and K_{di}. Further support for the involvement of structural fluctuations in acrylamide quenching of LADH comes from the observation that pressure modulation of kq is directly correlated to modulation of protein flexibility (*15*), a finding not readily explained in terms of a binding model.

Inspection of the crystallographic structure allows speculation about the actual routes of access of acrylamide to the aromatic ring of W314. In the region of the dimer interface, it is possible to discern two potential gates that could expose the chromophore to the solvent (Figure 7A). One is represented by a zipperlike arrangement of the side chains of Gly-311, Thr-313, Lys-315, and Gly-316 in adjacent β-strands at the subunit interface. It is a positively charged gate the opening of which would involve swinging apart of the side chains of Lys-315 and Thr-313 in opposite strands and perhaps limited opening of the two β-strands (partial subunit dissociation). It would seem to be a good candidate for the low-frequency gate ($\upsilon_1 \approx 40$ s^{-1}), characterized by a relatively weak temperature dependence. The Lys side chains are mobile, and charge repulsion between Lys groups on facing strands will tend to keep them apart. Further, because lowering the temperature facilitates hydration of the subunit interface area and tends to weaken subunit association, this gate is expected to maintain a good efficiency even at low temperatures. According to the *B*-factors, these "zipper" residues become considerably immobilized in the ternary coenzyme complex (Figure 7B), which might explain the effective blocking of the slow gate. The combination of kinetic (high viscosity) and thermodynamic (reduction of the surface area exposed to the solvent) effects of glycerol is also anticipated to achieve a substantial reduction in gate frequency. The other potential gate is a natural channel located near the dimer interface, roughly at 180° from the zipper (Figure 7A). This is a neutral gate blocked by the side chains of Val-276 and Leu- 307, which being hydrophobic will be driven in the low-hydration, closed state. As opening involves the rotation of side chains, it is potentially a high-frequency gate and, therefore, a plausible candidate for υ_2. Again, the *B*-factors indicate that the mobility of Val-276 and Leu-307 is severely restricted in the coenzyme complex, thereby predicting a sharp drop in the quenching rate from the apo- to holoprotein, as is observed. Equally, the viscous drag of glycerol is expected to slow these motions and reduce υ_2. Of course, these working hypotheses can be tested by site specific mutations, as recently reported for superoxide dismutase (*34*), although much can be learned about the nature of the gates also from the use of

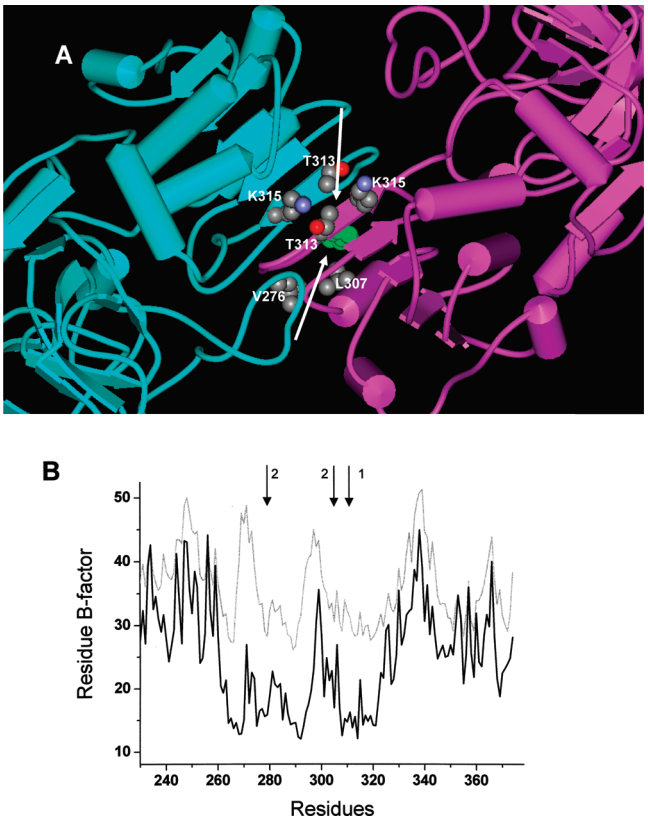

FIGURE 7: (A) Ribbon diagram representation of a recently published X-ray structure of LADH (Protein Data Bank entry 1YE3) with a detail of the dimer subunit interface. The arrows indicate two potential protein gates permitting acrylamide to penetrate into the vicinity of W314. Illustrated in CPK are the indole ring of W314 (green), the side chains of T313 and K315 in opposite β-strands at the interface (gate 1), and the V276−L307 pair of one subunit (gate 2). (B) Plot of the residue *B*-factors, for the polypeptide segment in the region of the dimer interface, as obtained from the X-ray structure of LADH (thin line, Protein Data Bank entry 1YE3) and of the ternary complex with NAD^+ and benzyl alcohol (thick line, Protein Data Bank entry 1HLD). The arrows point to the residues involved in the gates.

acrylamide derivatives varying in size and charge, which is the subject of ongoing investigations.

In summary, these results with LADH emphasize that quenching of the long-lived phosphorescence of internal Trp residues by relatively large quencher molecules may represent an important tool for disclosing protein-gated internal migration of solutes in the relatively slow ($\tau_0 = -10^{-5}$ s) time domain. Of particular interest are slow motions, such as transient partial unfolding transitions, that permit one to visit rarely populated conformational states that because of their rarity are beyond detection by most biophysical techniques. Whether these motions are directly involved in the diffusive penetration of enzyme substrates and cofactors, their detection is nevertheless valuable for unveiling dynamical aspects of the globular fold in a time domain where information is scarce. The method makes use of a natural probe that in principle can be placed in strategic regions of the macromolecule and that, by varying the size of Q, may enquire on local structural fluctuations over a wide range of frequencies and amplitudes.

SUPPORTING INFORMATION AVAILABLE

Variation of α_i and τ_i as a function of acrylamide concentration in a typical experiment. This material is available free of charge via the Internet at http://pubs.acs.org.

REFERENCES

1. Persson, E., and Halle, B. (2008) Nanosecond to microsecond protein dynamics probed by magnetic relaxation dispersion of buried water molecules. *J. Am. Chem. Soc. 130*, 1774–1787.
2. Eppler, R. K., Hudson, E. P., Chase, S. D., Dordick, J. S., Reimer, J. A., and Clark, D. S. (2008) Biocatalyst activity in nonaqueous environments correlates with centisecond-range protein motions. *Proc. Natl. Acad. Sci. U.S.A. 105*, 15672–15677.
3. Henzler-Wildman, K., and Kern, D. (2007) Dynamic personalities of proteins. *Nature 450*, 964–972.
4. Hammes-Schiffer, S., and Benkovic, S. J. (2006) Relating protein motion to catalysis. *Annu. Rev. Biochem. 75*, 519–541.
5. Kale, S., Ulas, G., Song, J., Brudvig, G. W., Furey, W., and Jordan, F. (2008) Efficient coupling of catalysis and dynamics in the E1 component of *Escherichia coli* pyruvate dehydrogenase multienzyme complex. *Proc. Natl. Acad. Sci. U.S.A. 105*, 1158–1163.
6. Bouvignies, G., Bernado, P., Meier, S., Cho, K., Grzesiek, S., Bruschweiler, R., and Blackledge, M. (2005) Identification of slow correlated motions in proteins using residual dipolar and hydrogen-bond scalar couplings. *Proc. Natl. Acad. Sci. U.S.A. 102*, 13885–13890.
7. Lakowicz, J. R., and Weber, G. (1973) Quenching of protein fluorescence by oxygen. Detection of structural fluctuations in proteins on the nanosecond time scale. *Biochemistry 12*, 4171–4179.
8. Eftink, M. R. (1991) in Topics in Fluorescence Spectroscopy (Lakowicz, J. R., Ed.) p v, Plenum Press, New York.
9. Strambini, G. B. (1987) Quenching of alkaline phosphatase phosphorescence by O_2 and NO. Evidence for inflexible regions of protein structure. *Biophys. J. 52*, 23–28.
10. Vanderkooi, J. M. (1991) in Topics in Fluorescence Spectroscopy (Lakowicz, J. R., Ed.) pp 113−132, Plenum Press, New York.
11. Cioni, P., and Strambini, G. B. (1998) Acrylamide quenching of protein phosphorescence as a monitor of structural fluctuations in the globular fold. *J. Am. Chem. Soc. 120*, 11749–11757.
12. Calhoun, D. B., Englander, S. W., Wright, W. W., and Vanderkooi, J. M. (1988) Quenching of room temperature protein phosphorescence by added small molecules. *Biochemistry 27*, 8466–8474.
13. Calhoun, D. B., Vanderkooi, J. M., and Englander, S. W. (1983) Penetration of small molecules into proteins studied by quenching of phosphorescence and fluorescence. *Biochemistry 22*, 1533–1539.
14. Cioni, P., Bramanti, E., and Strambini, G. B. (2005) Effects of sucrose on the internal dynamics of azurin. *Biophys. J. 88*, 4213–4222.
15. Cioni, P., and Strambini, G. B. (1999) Pressure/temperature effects on protein flexibilty from acrylamide quenching of protein phosphorescence. *J. Mol. Biol. 291*, 955–964.
16. Strambini, G. B., Kerwin, B. A., Mason, B. D., and Gonnelli, M. (2004) The triplet-state lifetime of indole derivatives in aqueous solution. *Photochem. Photobiol. 80*, 462–470.
17. Cioni, P., Gabellieri, E., Gonnelli, M., and Strambini, G. B. (1994) Heterogeneity of Protein Conformation in Solution from the Lifetime of Tryptophan Phosphorescence. *Biophys. Chem. 52*, 25–34.
18. Sillen, A., and Engelborghs, Y. (1998) The Correct Use of "Average" Fluorescence Parameters. *Photochem. Photobiol. 65*, 475–486.
19. Owen, C. S., and Vanderkooi, J. M. (1991) Diffusion-dependent and -independent collisional quenching of fluorescence and phosphorescence. *Comments Mol. Cell. Biophys. 7*, 235–257.
20. Vanderkooi, J. M., Englander, S. W., Papp, S., Wright, W. W., and Owen, C. S. (1990) Long-Range Electron Exchange Measured in Proteins by Quenching of Tryptophan Phosphorescence. *Proc. Natl. Acad. Sci. U.S.A. 87*, 5099–5103.
21. Szabo, A., Shoup, D., Northrup, S. H., and McCammon, J. A. (1982) Stochastically gated diffusion-influenced reactions. *J. Chem. Phys. 77*, 4484–4493.
22. Zhou, H.-X. (1998) Theory of the diffusion-influenced substrate binding rate to a buried and gated active site. *J. Chem. Phys. 108*, 8146–8154.
23. Somogyi, B., Norman, J. A., Punyiczki, M., and Rosenberg, A. (1992) Viscosity dependence of acrylamide quenching of ribonuclease T1 fluorescence. The gating mechanism. *Biochim. Biophys. Acta 1119*, 81–89.
24. Eklund, H., Samama, J. P., and Jones, T. A. (1984) Crystallographic investigations of nicotinamide adenine dinucleotide binding to horse liver alcohol dehydrogenase. *Biochemistry 23*, 5982–5986.
25. Ramaswamy, S., Eklund, H., and Plapp, B. V. (1994) Structures of horse liver alcohol dehydrogenase complexed with NAD^+ and substituted benzyl alcohols. *Biochemistry 33*, 5230–5237.
26. Strambini, G. B., and Gonnelli, M. (1990) Tryptophan Luminescence from Liver Alcohol-Dehydrogenase in Its Complexes with Coenzyme: A Comparative Study of Protein Conformation in Solution. *Biochemistry 29*, 196–203.

27. Theorell, H., and Tatemoto, K. (1971) Thermal stability of horse liver alcohol dehydrogenase and its complexes. *Arch. Biochem. Biophys. 143*, 354–358.
28. Gekko, K., and Timasheff, S. N. (1981) Thermodynamic and kinetic examination of protein stabilization by glycerol. *Biochemistry 20*, 4677–4686.
29. Punyczki, M., Norman, J. A., and Rosenberg, A. (1993) Interaction of acrylamide with proteins in the concentration range used for fluorescence quenching studies. *Biophys. Chem. 47*, 9–19.
30. Kerwin, B. A., Chang, B. S., Gegg, C. V., Gonnelli, M., Li, T. S., and Strambini, G. B. (2002) Interactions between PEG and type I soluble tumor necrosis factor receptor: Modulation by pH and by PEGylation at the N terminus. *Protein Sci. 11*, 1825–1833.
31. Gavish, B. (1980) Position-dependent viscosity effect on rate coefficient. *Phys. Rev. Lett. 44*, 1160–1163.
32. Gavish, B., and Werber, M. M. (1979) Viscosity-dependent structural fluctuations in enzyme catalysis. *Biochemistry 18*, 1269–1275.
33. Marcus, R. A., and Sutin, N. (1985) Electron transfer in chemistry and biology. *Biochim. Biophys. Acta 811*, 265–322.
34. Whittaker, M. M., and Whittaker, J. W. (2008) Conformationally gated metal uptake by apomanganese superoxide dismutase. *Biochemistry 47*, 11625–11636.